Journal of Materials Chemistry

www.rsc.org/materials

Volume 21 | Number 30 | 14 August 2011 | Pages 11013–11440

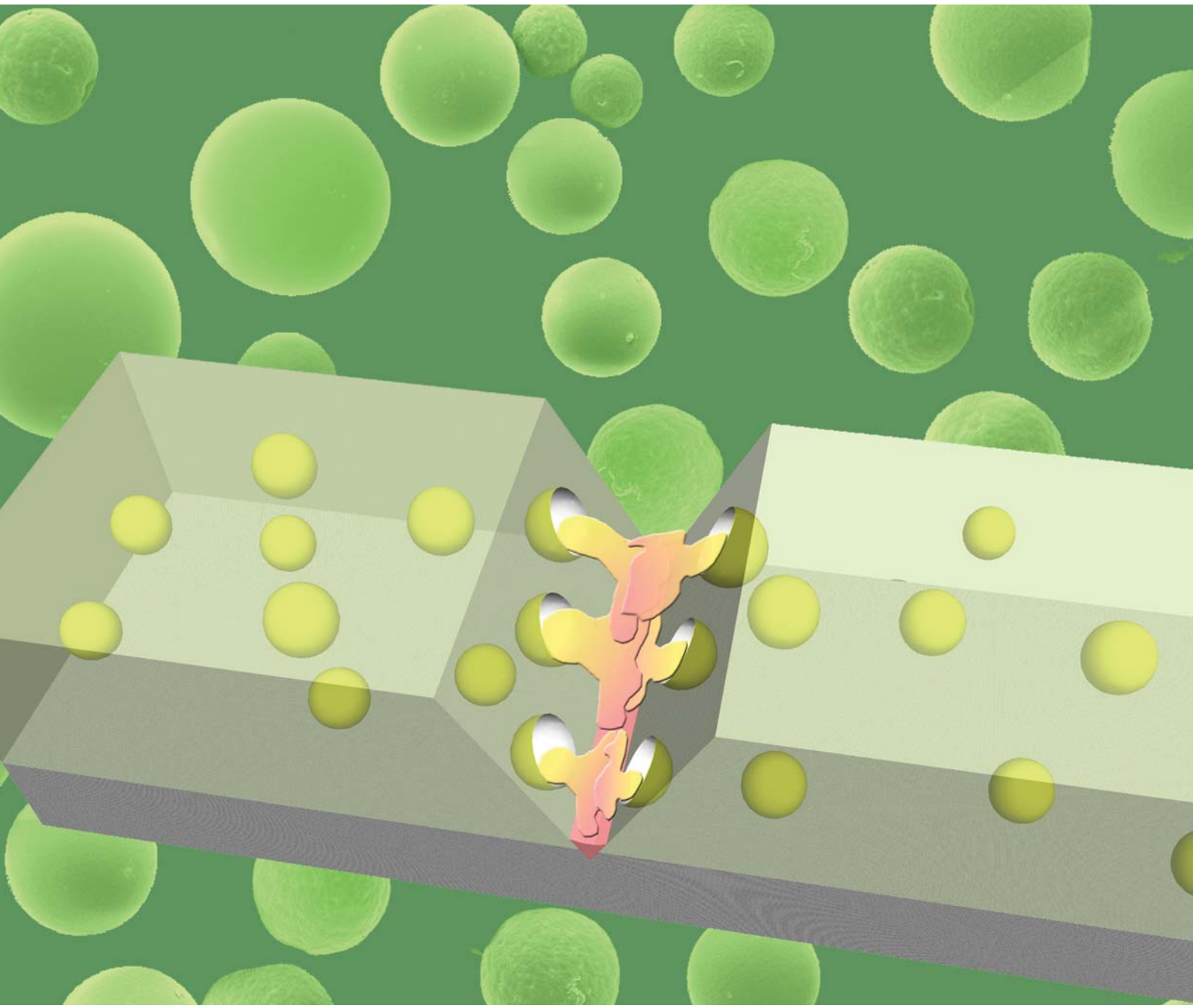

ISSN 0959-9428

RSC Publishing

PAPER

Mingxing Huang and Jinglei Yang

Facile microencapsulation of HDI for self-healing anticorrosion coatings

Journal of Materials Chemistry

Dynamic Article Links

Cite this: *J. Mater. Chem.*, 2011, **21**, 11123

www.rsc.org/materials

PAPER

Facile microencapsulation of HDI for self-healing anticorrosion coatings

Mingxing Huang and Jinglei Yang*

Received 23rd February 2011, Accepted 17th May 2011
DOI: 10.1039/c1jm10794a

Published on 30 June 2011 on http://pubs.rsc.org | doi:10.1039/C1JM10794A
Downloaded on 01 August 2011

Polyurethane (PU) microcapsules containing hexamethylene diisocyanate (HDI) as core materials are facilely manufactured *via* interfacial polymerization reaction of commercial methylene diphenyl diisocyanate (MDI) prepolymer and 1,4-butanediol in an oil-in-water emulsion. The resultant capsules have diameters of 5–350 μm and shell thickness of 1–15 μm, both linearly related to the agitation rate in the double logarithm coordinates. The typical core fraction of microcapsules and the yield of synthesis are around 60 wt% and 70 wt%, respectively, while varying with reaction conditions. The effects of parameters including reaction duration and temperature, surfactant concentration, agitation rate, and environmental factors on the formation of microcapsules were systematically investigated and optimized. Quality assessments of each batch of microcapsules were performed using thermogravimetric analysis and scanning electron microscopy. Anticorrosion coatings mixed with synthesized microcapsules were prepared on a steel substrate. Preliminary results indicated significant corrosion retardancy happened in the self-healing coatings under an accelerated corrosion process, showing the great potential of this facile microencapsulation technique in development of catalyst-free, one-part self-healing coatings for corrosion control.

1. Introduction

Self-healing materials have received considerable attention due to their great potential to diminish degradation and reduce the maintenance cost.[1–7] Since the first generation self-healing material based on the ring opening metathesis polymerization (ROMP) of encapsulated dicyclopentadiene (DCPD) in the presence of Grubbs' catalyst particles,[8] microencapsulation has been one of the most efficient and widely used approaches in self-healing materials development. Poly(urea-formaldehyde) (PUF) microcapsules containing DCPD as healing agent were prepared through an *in situ* polymerization in oil-in-water emulsion,[9,10] and the capsules size was further reduced to nanometre scale with the assistance of a sonication technique.[11] Linseed oil,[12] amines[13] and epoxy resins[14] were also microencapsulated for self-healing applications. To avoid the contamination of catalyst by the host matrix, a dual-capsule system was reported,[15,16] and this approach has shown good self-healing and corrosion protection features. To our knowledge, most of the capsules applied for self-healing purpose were made from PUF, polyurethane (PU) and polyurea. To overcome this limitation, a double-walled polyurethane-poly(urea-formaldehyde) (PU-PUF) microcapsule was recently developed through the combination of interfacial polymerization of PU and *in situ* polymerization of PUF in a single batch reaction.[17] Other approaches such as hollow glass fiber embedment,[18–20] microvascular system,[21,22] and electrospun hollow fibers[23] have also been extensively investigated for self-healing materials development, and more recently there was reported an oxetane-substituted chitosan precursor incorporated PU showing good scratch closure performance within half an hour under sunlight.[24]

Isocyanates are reactive with moisture, and can be used as a potential healing agent to develop one-part, catalyst-free self-healing materials that are exposed to moist or aqueous environments. On the other hand, however, the high reactivity of isocyanates brings the difficulty for processing. Previous research on encapsulation of isocyanate has been mainly restricted to its blocked form or solid state.[25,26] Yang *et al.*[27] for the first time reported the microencapsulation of liquid isocyanate monomer. Less reactive isophorone diisocyanate (IPDI) was encapsulated by PU microcapsules based on the polymerization of toluene diisocyanate (TDI) prepolymer that was cautiously in-house synthesized.[27]

Here we report a significant improvement of a facile microencapsulation approach for liquid isocyanates. More reactive HDI monomer is microencapsulated *via* an interfacial polymerization method in oil-in-water emulsion, which makes the instant healing possible. In addition, commercially available MDI based prepolymer is used to form capsule shell, which makes it ready for mass production of microcapsules.

2. Experimental

2.1. Materials

MDI prepolymer Suprasec 2644 was obtained from Huntsman. HDI, gum arabic, 1,4-butanediol, ethylenediamine and sodium

School of Mechanical and Aerospace Engineering, Nanyang Technological University, Singapore, 639798. E-mail: mjlyang@ntu.edu.sg; Fax: +65 6792 4062; Tel: +65 6790 6906

Published on 30 June 2011 on http://pubs.rsc.org | doi:10.1039/C1JM10794A
Downloaded on 01 August 2011

chloride (NaCl) were obtained from Sigma-Aldrich. All chemicals in this study were used without further purification unless otherwise specified.

2.2. Synthesis of microcapsules containing HDI

The microcapsules preparation was based on the interfacial polymerization reaction of Suprasec 2644 and 1,4-butanediol in an oil-in-water emulsion system. At room temperature, gum arabic aqueous solution was prepared as surfactant in a 250 ml beaker. The beaker was suspended in a temperature-controlled water bath on a programmable hot plate with an external temperature probe. The solution was agitated with a digital mixer (Caframo) driving a three-bladed propeller. 2.9 g of Suprasec 2644 liquid was mixed well with HDI, and the mixture was then added into the prepared surfactant solution under agitation to develop a stable emulsion system. After the addition, the system was heated to the set temperature at the heating rate of 7 °C min^{-1}, and diluted solution of 3.0 g of 1,4-butanediol was dropwisely added into the emulsion to initiate the interfacial polymerization at the oil/water interface. The reaction was stopped after a certain period of time, and the resultant microcapsules were filtered and washed with distilled water for several times. Microcapsules were collected for air-drying at room temperature for 48 h before further analysis.

2.3. Morphology and statistic parameters of HDI microcapsules

The microcapsule formation during the reaction process was observed under an Axiotech optical microscope (Zeiss) equipped with a device camera (Sony). The surface morphology and shell thickness were examined by using scanning electron microscopy (JEOL JSM 5600LV SEM). Mean diameter of the microcapsules and their size distribution were determined from data sets of at least 200 measurements from SEM images and analyzed in ImageJ.

2.4. Yield and components of HDI microcapsules

Since the synthesis of the capsule shell wall is not a strict stoichiometric reaction, excess of 1,4-butanediol was used to ensure the Suprasec 2644 was completely consumed, and the yield of the synthesis is calculated simply as below:

$$\text{Yield } (\%) = \frac{W_{cap}}{W_{pre\text{-}p} + W_{diol} + W_{HDI}} \times 100\%$$

where W_{cap} is the mass of the collected microcapsules after drying, and $W_{pre\text{-}p}$, W_{diol}, W_{HDI} are the masses of prepolymer, butanediol, and HDI, respectively. This is a rough method to compare the operating factor of the raw materials, which will bring more deviation at higher agitation rates and be explained in the latter section.

Constituents of the microcapsules were analyzed by using Fourier Transform Infrared Spectroscopy (FTIR, Varian 3100). Small amounts of pure HDI, pure prepolymer, pure capsule shell, pure capsule core material and full capsules mixed with KBr pellet were prepared separately. The spectrum in the range of 400 cm^{-1} to 4000 cm^{-1} was used for the observation. In order to obtain the FTIR spectrum of pure capsule shell, small amounts of microcapsules were crushed and washed by ethanol for a few times. After filtration and drying, pure shell was obtained for analysis.

2.5. Thermal property and core fraction of HDI microcapsules

The thermal stability and the HDI content of the resultant microcapsules were characterized by using thermogravimetric analysis (TGA, Hi-Res Modulated TGA 2950). 10–20 mg of microcapsules was put in a platinum pan and heated under nitrogen atmosphere at a rate of 10 °C min^{-1}. The peak width of the derivative of the weight loss curve of capsules was used to roughly determine the core fraction of microcapsules. Pure capsules shell was obtained using the same way as that for FTIR analysis.

2.6. Preparation and observation of anticorrosion self-healing coatings

Anticorrosion self-healing coatings were prepared by dispersing 10 wt% of synthesized microcapsules into epoxy resin (EPOLAM 5015/5014, AXSON) at ambient temperature, followed by mixing hardener. The mixture was then placed under vacuum for degassing for 20 min. A steel panel was polished by sand paper, degreased by acetone, and then washed by distilled water. After drying, the panel was coated by the degassed self-healing coating with the final thickness of 300–350 μm. After curing, cross scratches were applied manually on the coating by razor blade. Pure epoxy coating was prepared as a control. Specimens coated with both formulations were immersed in 10 wt% NaCl solution for 48 h to evaluate the accelerated corrosion process.

Optical photography was used to observe the different corrosion performances of the steel panel coated with self-healing coating and with neat epoxy coating. SEM was also employed to inspect the evolution of the scratched area of the coating to provide detailed information about the corrosion process.

3. Results and discussion

3.1. Overview of the synthesized microcapsules

In the synthesis, Suprasec 2644 was dissolved in HDI to yield an oil phase, which was dispersed into gum arabic surfactant solution to generate an oil-in-water emulsion. When 1,4-butanediol was introduced, the primary polymerization reaction between the hydroxyl functional group of this diol in the aqueous phase and isocyanate functional group in the oil phase would take place at the oil/water interface to produce a polymeric membrane surrounding the oil droplets. The diol in the aqueous phase thereafter diffused across the initial membrane to react with the isocyanates and resulted in the membrane increment.[28] MDI prepolymer was much more reactive than HDI, and hence the primary reaction was between 1,4-butanediol and prepolymer to form the shell structure, while the relatively less reactive HDI liquid was encapsulated as core material to produce the final microcapsules. In addition, there were a few side reactions between NCO groups from prepolymer, HDI, and intermediate polyisocyanates and hydroxyl groups from diol and water. Among those, the side reaction for example between reactive NCO groups and water would eventually produce a mixture of polyurethane and polyurea as shell wall. Actually some bubbles were observed upon the completion of the microencapsulation process, indicating carbon dioxide was

 This journal is © The Royal Society of Chemistry 2011

Published on 30 June 2011 on http://pubs.rsc.org | doi:10.1039/C1JM10794A
Downloaded on 01 August 2011

produced in the side reaction between NCO groups and water. However, to identify the precise chemical compositions of the shell wall material is beyond the scope of this study.

In a typical run of synthesis, the microcapsules were obtained by adding 8 g of HDI in 3 wt% gum arabic solution at the agitation rate of 500 RPM and the temperature of 40 °C and reacting for 1 h. At such a condition, the yield of the capsules was about 70 wt%, and the resultant microcapsules had average diameter of 86.5 μm and shell thickness of about 6.5 μm.

3.1.1 Morphology. The nearly spherical shaped microcapsules were synthesized with size distribution as shown in Fig. 1a. It is seen that the outer surface of the capsules is quite smooth (Fig. 1c) compared with those synthesized using other approaches.[9,27] Meanwhile, the shell wall thickness is roughly uniform and in the micron meter level, which acts as an appropriate barrier from leakage and provides enough mechanical stiffness from rupture during post processing.

3.1.2 Yields and determination of capsule components. According to the calculation discussed above, at 500 RPM agitation rate, the typical yield was around 70 wt%. A more detailed analysis is given in the next section to show that the product yield was slightly dependent on agitation rate.

The chemical structure of the resultant microcapsules was characterized by FTIR. For comparison, complete capsules together with pure grades of HDI, prepolymer, shell and core materials were investigated, as shown in Fig. 2. The nearly identical spectrum curves of HDI and core material indicated that HDI was successfully encapsulated and no MDI prepolymer was included since the signal peaks at 1641.5 cm^{-1}, 1540.7 cm^{-1} were not detected. From the spectrum of shell, the characteristic signal at 2267.6 cm^{-1} (–NCO stretch) was not observed, indicating the prepolymer chains were extended to form polyurethane bulk shell. Large amounts of HDI monomer released upon squeezing the microcapsules indicated that HDI played a minor role in the shell forming process. From the large –NCO stretching peak of the spectrum of complete capsules, it was logical to confirm again that HDI was encapsulated.

3.1.3 Thermal property and core fraction of microcapsules. The TGA weight loss curves of microcapsules synthesized at 500 RPM along with pure HDI and capsule shell material as a function of temperature are shown in Fig. 3. It can be observed that microcapsules experienced significant weight loss by 180 °C, which is in good agreement with that of pure HDI, revealing the successful encapsulation of HDI within the microcapsules. The decomposition of shell materials started from about 240 °C.

The derivative of the weight loss curve of microcapsules was also plotted in Fig. 3, clearly showing the evaporation process of HDI in the first peak and decomposition process of shell in the peaks after 240 °C. From the peak width of the derivative curve, the core fraction of the microcapsules was determined to be around 62% at 500 RPM.

3.1.4 Reactivity of core material. When the resultant microcapsules were crushed between two microscope slides, a large amount of liquid was observed to be released with irritating odor. After addition of a few droplets of ethylenediamine, it was found that the released liquid hardened rapidly with the production of heat, indicating that the encapsulated HDI was still reactive. When the core material was released on a moist glass slide, a whitish solid polymer layer appeared after a few hours, indicating the potential for self-healing application especially in a humid environment.

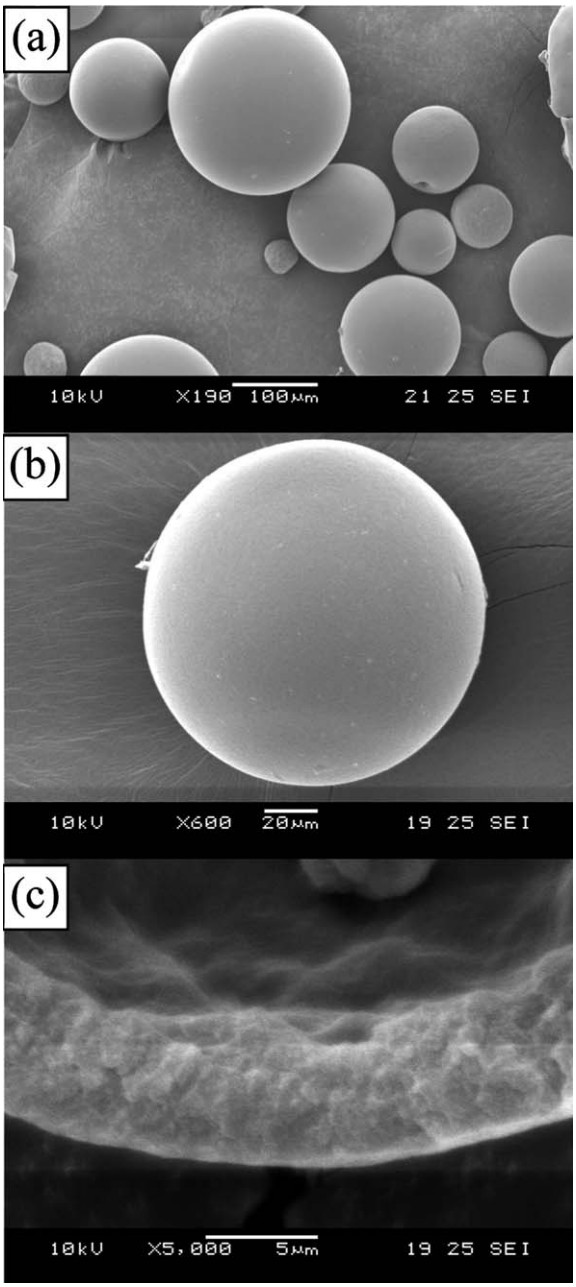

Fig. 1 Morphology of microcapsules. (a) Spherical shaped microcapsules, (b) zoomed in image showing smooth outer surface, and (c) shell wall profile.

3.2. Parametric study and optimal microencapsulation procedure

3.2.1 Determination of minimum reaction time (MRT). The formation of microcapsules was rather fast in the synthesis due to

Published on 30 June 2011 on http://pubs.rsc.org | doi:10.1039/C1JM10794A
Downloaded on 01 August 2011

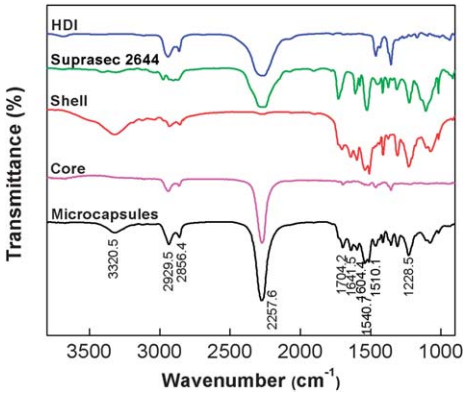

Fig. 2 FTIR spectra of prepared microcapsules, capsules shell, capsule core, Suprasec 2644 and HDI.

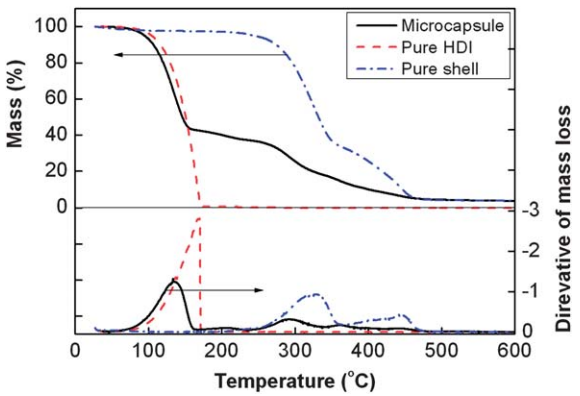

Fig. 3 TGA weight loss of pure HDI and prepared microcapsules, and the derivative of TGA curve of microcapsules.

the high reactivity of MDI prepolymer. Optical microscopy (OM) examination during the reaction period showed that microcapsules formed within 15 min after the addition of 1,4-butanediol. However, the MRT was necessary to know for both time saving and quality control of shell wall. To determine the MRT, products were sampled from the emulsion solution at 10 min intervals and observed under microscope until dispersed dry microcapsules could be collected following normal product collection operation. Although microcapsules were observed at quite early stage, the capsules formed before the MRT were found to collapse to yield viscous bulky polymer during the filtration. The required MRT at different reaction temperature was plotted in Fig. 4, and it can be seen that the MRT reduced steadily from 150 min to 30 min when the reaction temperature increased from 30 °C to 60 °C, respectively.

3.2.2 Optimal reaction temperature. Reaction temperature had considerable influence on the core content in the resultant microcapsules. As shown in Fig. 4, the core fraction increased from 18% to 65% when the reaction temperature was reduced from 60 °C to 30 °C during the capsules synthesis. This variation in the core fraction was probably due to the side reactions between 1,4-butanediol and HDI, and water and NCO groups. As discussed above, the shell materials were primarily based on the reaction of 1,4-butanediol with MDI prepolymer, but the

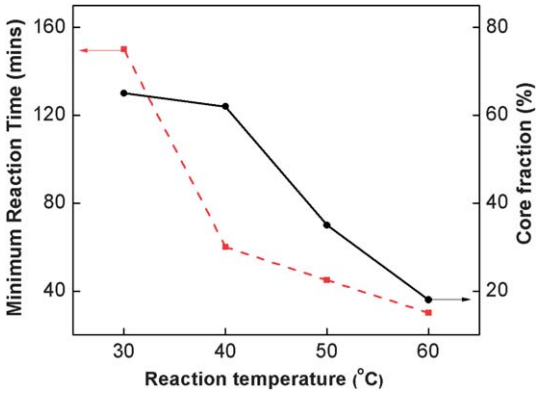

Fig. 4 MRT for the synthesis and core fraction of prepared microcapsules as a function of reaction temperature.

reaction with less reactive HDI was also unavoidable especially at elevated temperature. In addition, at high temperature water molecules might easily diffuse into capsules and react with HDI to produce polyurea *via* the intermediate product of amines and carbon dioxide. By consideration of most robust microcapsules with highest core content synthesized in minimum reaction time, it was reasonable to choose 40 °C as the optimal reaction temperature from our study.

3.2.3 Initial mass of core material. The core material content of microcapsules can also be controlled by adjusting the amount of HDI in the recipe. As illustrated in Fig. 5, higher fill content in the final capsules was obtained when more HDI was added, showing a nonlinear relationship. It is a natural process that when more oil phase is dispersed into aqueous solution, more oil droplets are formed. However, there will be an optimal value to obtain robust microcapsules since the amount of shell materials is constant. A direct consequence of using more HDI was that more aggregation microcapsules appeared with bad quality although core content was a bit higher. This observation was in accordance with a previous investigation.[29]

3.2.4 Influence of surfactant concentration

On geometries of microcapsules. The concentration of surfactant greatly influenced the diameter of the resultant

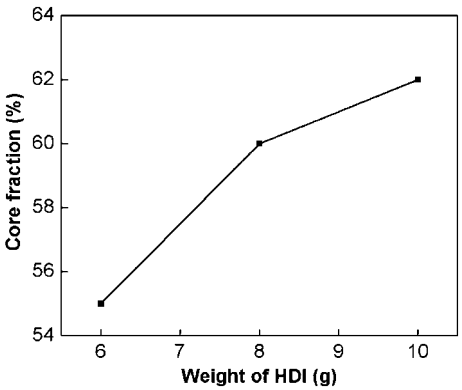

Fig. 5 Core fraction of microcapsule as a function of the amount of HDI in the recipe.

This journal is © The Royal Society of Chemistry 2011

Published on 30 June 2011 on http://pubs.rsc.org | doi:10.1039/C1JM10794A
Downloaded on 01 August 2011

microcapsules. As shown in Fig. 6, microcapsules diameter decreased dramatically when the gum arabic concentration increased from 1.5 to 3 wt%, followed by a plateau with constant diameter around 85 μm when the surfactant concentration was above 3 wt%. The exact mechanism by which surfactant concentration influences the capsules formation is still not clear, but it is widely accepted that the surfactant concentration is a dominant factor influencing the interfacial tension of the emulsion media before the critical micelle concentration (CMC) is reached.[30,31] It is believed that higher surfactant concentration yields smaller oil droplets in an oil-in-water emulsion, and as a result, the microcapsules produced *via* interfacial reaction will have smaller diameters.[32] Beyond the CMC, further increase in surfactant concentration will not change the interfacial tension and the size of dispersed droplets in the emulsion system, and therefore the diameter of final microcapsules will approximately maintain a constant value. From our system, it was indicated that the CMC of gum arabic was around 3 wt%.

On core fraction of microcapsules. Although surfactant concentration significantly influenced the capsules diameter, it only slightly affected the core fraction. As compared in Fig. 6, the HDI fraction in the final microcapsules changed from 58% to 63% when the gum arabic concentration varied in the range of 1.5–10 wt%.

3.2.5 Influence of agitation rate

On yields of microcapsules. It was found that the yields of microcapsules varied from 74 to 54 wt% when the agitation rates ranged from 300 to 2000 RPM, respectively, as shown in Fig. 7. It is likely attributable to two reasons. First of all, more microcapsules after formation might be destroyed by the higher shear force under faster agitation.[9] Secondly, during the product collection, a large portion of tiny capsules were not collected in the process of filtration and washing. As discussed below, we can find that a finer microcapsule will be produced at higher agitation rate, and accordingly more tiny capsules would escape from our collection, resulting in the lower yield. As mentioned above, the yield calculation was a rough estimation. The yield at 2000 RPM agitation rate was approximately 54%.

On geometries of microcapsules. In the development of self-healing materials through microencapsulation, proper control of

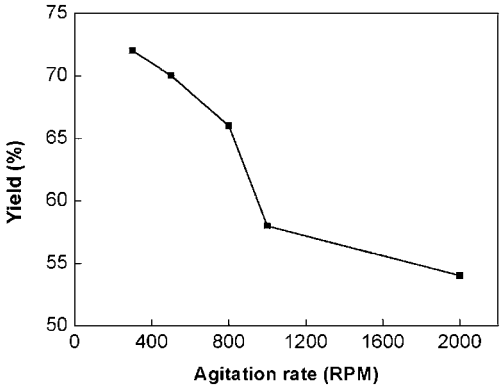

Fig. 7 Yield of microcapsules *vs.* agitation rate.

capsule diameter is a key issue because the diameter greatly influences the self-healing performance,[33] and in some conditions, only the capsules with a given range of diameters are suitable. The microcapsules diameter is influenced by a combination of several factors including the geometry of the mixing device, viscosity of the reaction media, surfactant concentration, agitation rate, temperature, *etc.*, and from the above discussions, it was seen that the gum arabic concentration greatly influenced the microcapsules size. However, the average diameter of microcapsules was primarily controlled by the agitation rate after all other parameters were optimized. As illustrated in Fig. 8 and 9, higher agitation speed resulted in smaller microcapsule size and narrower size distribution, and this result was in line with those previously reported.[9,27] At higher agitation rate, finer oil droplets formed in the emulsion system due to the stronger shear force, and the final microcapsules were accordingly smaller. Meanwhile, faster agitation was more favorable for the homogenization of the emulsion, and therefore the diameter distribution of the produced microcapsules was more uniform. Microcapsules with average diameter in the range of 5–350 μm were obtained by adjusting agitation rate from 300 to 2000 RPM. The relation between average diameter and agitation was linear in the double logarithm coordinates, similar to the previous research.[9]

The average shell thickness of the resultant microcapsules as a function of agitation rate was also plotted in Fig. 8, which

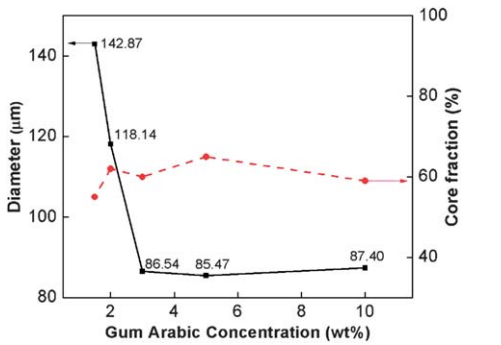

Fig. 6 Diameter and core fraction of microcapsules prepared at different concentration of gum arabic.

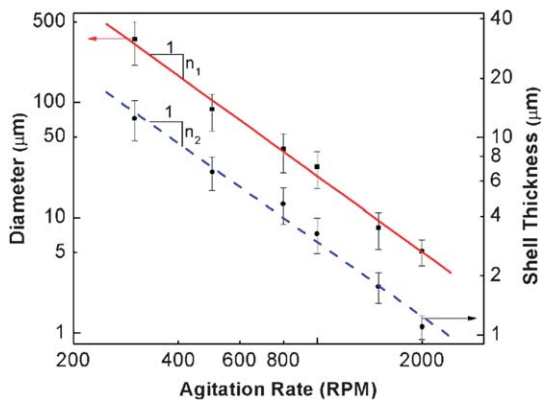

Fig. 8 Diameter and shell thickness of microcapsules prepared at different agitation rate ($n_1 = 2.18$; $n_2 = 1.25$).

Published on 30 June 2011 on http://pubs.rsc.org | doi:10.1039/C1JM10794A
Downloaded on 01 August 2011

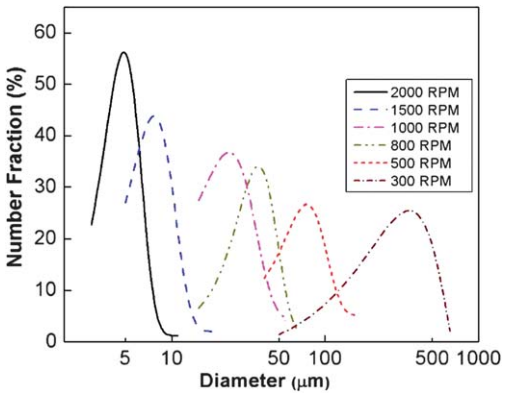

Fig. 9 Size distributions of microcapsules prepared at different agitation rates.

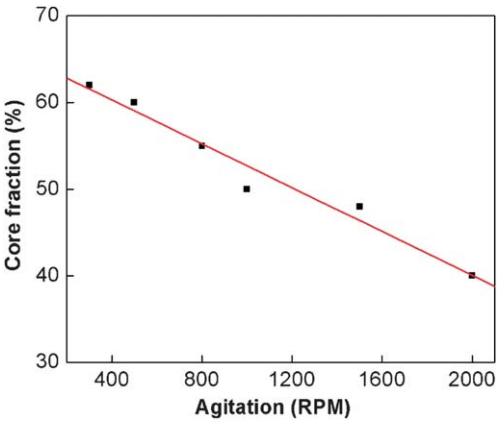

Fig. 10 Core fraction of microcapsules prepared at different agitation rate.

clearly illustrated that the shell thickness reduced with the increase of agitation rate following a linear relation in double logarithm coordinates. As stated above, finer oil droplets were generated at higher agitation rate, and their specific surface area was larger. Given the total amount of core materials and shell materials remained constant, the amount of shell materials surrounding each oil droplet would therefore be smaller, resulting in the thinner shell wall of the final microcapsules. The average shell thickness of capsules was in the range of 1.1–12.5 μm when the agitation rate varied from 300 to 2000 RPM. The relation between average diameter and agitation rate was consistent with the previous observations.[27]

On core fractions of microcapsules. The agitation rate also influenced the core fractions of the resultant microcapsules. As shown in Fig. 10, faster agitation led to lower core fractions, and the HDI content in the capsules reduced from 62% to 40% when the agitation rate was increased from 300 to 2000 RPM. The reason might be that the diffusion of 1,4-butanediol and maybe water across the thinner capsule shells produced at higher agitation rates was easier and accordingly more HDI reacted with the diol. As a result, the core fraction in the final capsules was lower at higher agitation rate.

3.3. Environmental stability of HDI microcapsules

3.3.1 In aqueous solution. To investigate the stability of these capsules in a wet environment, the capsules were analyzed by TGA after they were immersed in water for a period of time. As revealed in Fig. 11, the core fraction reduced steadily with the immersion time and dropped to zero after 48 h immersion. The probable reason was that water diffused across the microcapsule wall and reacted with the encapsulated HDI, which was further proved by the SEM images of the change of the core morphology of microcapsules after immersion. As shown in Fig. 12, the core materials were solidified and eventually formed solid beads (Fig. 12b).

3.3.2 Shelf life. When the microcapsules were exposed to the open air at room temperature for 1 month, the HDI content dropped from 60% to 45%. This observation showed the high permeability of the microcapsules, and further optimization is still required to minimize the permeability in order to better protect the encapsulated core materials.

3.4. Preliminary self-healing performance in anticorrosion coating

The prepared microcapsules were integrated into an epoxy resin to create a self-healing coating, and a preliminary test was carried out to evaluate the self-healing and anti-corrosion performance. It can be seen from Fig. 13 that the scratched area of the steel panel coated with self-healing coating was nearly fully free of corrosion after 48 h immersion in salt solution. In contrast, severe corrosion was seen in the control specimen. This result clearly demonstrated the excellent corrosion protection of the prepared coating towards the steel panel. From the SEM images of the scratched area of the coated panels (Fig. 14), it was illustrated that newly formed materials filled the crack. The crack was in this way sealed and healed autonomously to retard the diffusion of salt ions and thus protect the substrate from the corrosion process. The materials generated in the crack should be the product between HDI released from ruptured microcapsules and water. As a comparison, it could be seen that the crack of the control specimen was not sealed and severe rust was observed. Therefore, it could be concluded that the anti-corrosion function

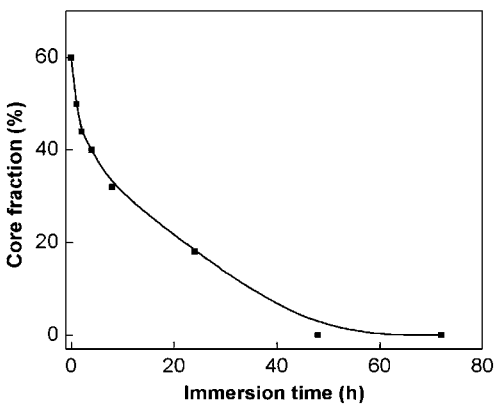

Fig. 11 Core fraction of microcapsules after immersion in water for different time.

This journal is © The Royal Society of Chemistry 2011

Published on 30 June 2011 on http://pubs.rsc.org | doi:10.1039/C1JM10794A
Downloaded on 01 August 2011

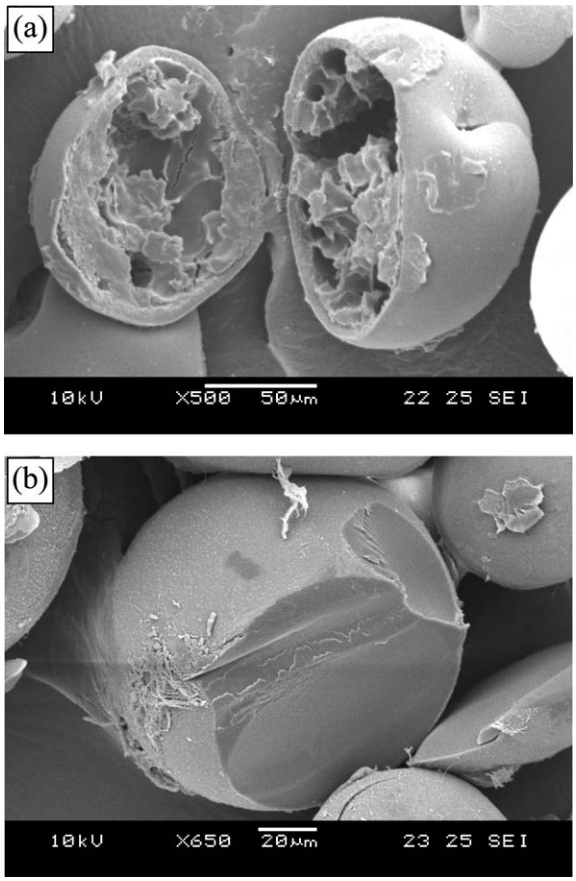

Fig. 12 SEM images of microcapsules after (a) 24 h and (b) 48 h immersion in 10% NaCl aqueous solution.

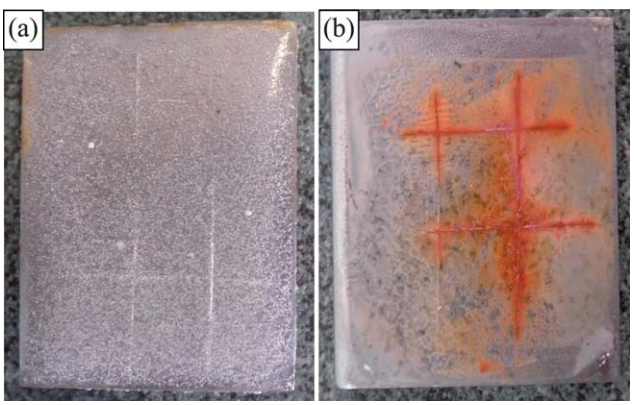

Fig. 13 Corrosion test results for steel panels coated with (a) epoxy coating mixed with 10 wt% of prepared HDI-filled microcapsules; (b) control epoxy coating. The panels were immersed in 10% NaCl solution for 48 h.

of the coating is from its self-healing property. The healing behavior of the microcapsules-embedded epoxy coating was completely autonomous without any external intervention such as heating or UV exposure, and it did not require catalyst or other assisting materials either, making it easier for the development of self-healing materials, which is of considerable technical and commercial importance.

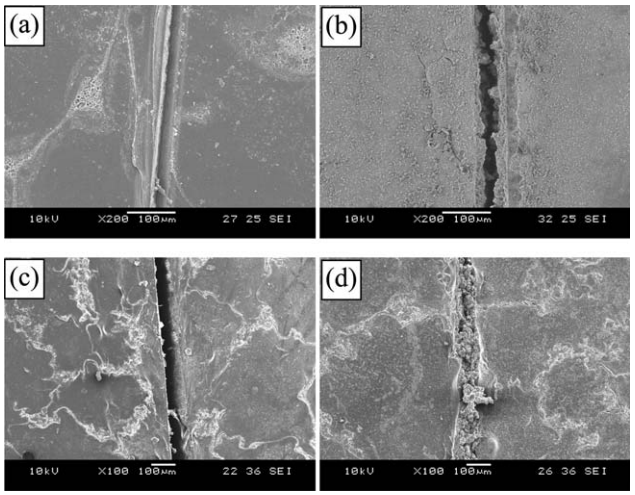

Fig. 14 SEM images of the scratched regions before immersion (a: control coating, c: self-healing coating) and after immersion in salt water for 48 h (b: control coating, d: self-healing coating).

4. Conclusion

A procedure for optimal microencapsulation of HDI *via* interfacial polymerization reaction of MDI prepolymer and 1,4-butanediol in an oil-in-water emulsion was facilely achieved for self-healing application. The yield of the synthesis was about 70% and dependent on reaction parameters. Spherical microcapsules with the diameter in the range of 5–350 μm and shell thickness in the range of 1–15 μm were prepared by adjusting agitation rate from 300 to 2000 RPM. The average diameter and shell thickness of the microcapsules both possessed a linear relationship with agitation rate in double logarithm coordinates. HDI content of the resultant capsules was around 60 wt%, and it was inversely related to the reaction temperature. Microcapsules incorporated epoxy coating on a steel substrate showed excellent corrosion protection under an accelerated corrosion process *via* a self-sealing/healing mechanism, revealing the great potential of this facile microencapsulation technique in development of catalyst-free, one-part self-healing coatings for corrosion control.

Acknowledgements

The authors greatly acknowledge the financial support from Singapore MoE Tier 1 research fund (Grant #: RG17/09).

References

1 S. van der Zwaag, *Self healing materials: an alternative approach to 20 centuries of materials science*, Springer Verlag, 2007.
2 R. Trask, H. Williams and I. Bond, *Bioinspir. Biomimetics*, 2007, **2**, P1–P9.
3 D. Y. Wu, S. Meure and D. Solomon, *Prog. Polym. Sci.*, 2008, **33**, 479–522.
4 R. P. Wool, *Soft Matter*, 2008, **4**, 400–418.
5 S. Ghosh, *Self-healing materials: fundamentals, design strategies, and applications*, Wiley-VCH, 2009.
6 J. Syrett, C. Becer and D. Haddleton, *Polym. Chem.*, 2010, **1**, 978–987.
7 B. J. Blaiszik, S. L. B. Kramer, S. C. Olugebefola, J. S. Moore, N. R. Sottos and S. R. White, *Annu. Rev. Mater. Res.*, 2010, **40**, 179–211.

Published on 30 June 2011 on http://pubs.rsc.org | doi:10.1039/C1JM10794A
Downloaded on 01 August 2011

8 S. R. White, N. R. Sottos, P. H. Geubelle, J. S. Moore, M. R. Kessler, S. R. Sriram, E. N. Brown and S. Viswanathan, *Nature*, 2001, **409**, 794–797.
9 E. Brown, M. Kessler, N. Sottos and S. White, *J. Microencapsulation*, 2003, **20**, 719–730.
10 M. R. Kessler, N. R. Sottos and S. R. White, *Composites, Part A*, 2003, **34**, 743–753.
11 B. J. Blaiszik, N. R. Sottos and S. R. White, *Compos. Sci. Technol.*, 2008, **68**, 978–986.
12 C. Suryanarayana, K. C. Rao and D. Kumar, *Prog. Org. Coat.*, 2008, **63**, 72–78.
13 D. A. McIlroy, B. J. Blaiszik, M. M. Caruso, S. R. White, J. S. Moore and N. R. Sottos, *Macromolecules*, 2010, **43**, 1855–1859.
14 L. Yuan, G. Liang, J. Xie, L. Li and J. Guo, *Polymer*, 2006, **47**, 5338–5349.
15 S. Cho, H. Andersson, S. White, N. Sottos and P. Braun, *Adv. Mater.*, 2006, **18**, 997–1000.
16 S. H. Cho, S. R. White and P. V. Braun, *Adv. Mater.*, 2009, **21**, 645–649.
17 M. M. Caruso, B. J. Blaiszik, H. Jin, S. R. Schelkopf, D. S. Stradley, N. R. Sottos, S. R. White and J. S. Moore, *ACS Appl. Mater. Interfaces*, 2010, **2**, 1195–1199.
18 J. W. C. Pang and I. P. Bond, *Compos. Sci. Technol.*, 2005, **65**, 1791–1799.
19 R. Trask and I. Bond, *Smart Mater. Struct.*, 2006, **15**, 704–710.
20 H. Williams, R. Trask and I. Bond, *Smart Mater. Struct.*, 2007, **16**, 1198–1207.
21 A. Bejan, S. Lorente and K. M. Wang, *J. Appl. Phys.*, 2006, **100**, 033528.
22 K. Toohey, N. Sottos, J. Lewis, J. Moore and S. White, *Nat. Mater.*, 2007, **6**, 581–585.
23 J.-H. Park and P. V. Braun, *Adv. Mater.*, 2010, **22**, 496–499.
24 B. Ghosh and M. Urban, *Science*, 2009, **323**, 1458–1460.
25 I. W. Cheong and J. H. Kim, *Chem. Commun.*, 2004, 2484–2485.
26 H. Yang, S. Mendon and J. Rawlins, *eXPRESS Polym. Lett.*, 2008, **2**, 349–356.
27 J. Yang, M. W. Keller, J. S. Moore, S. R. White and N. R. Sottos, *Macromolecules*, 2008, **41**, 9650–9655.
28 P. Ni, M. Zhang and N. Yan, *J. Membr. Sci.*, 1995, **103**, 51–55.
29 H. Johnsen and R. B. Schmid, *J. Microencapsulation*, 2007, **24**, 731–742.
30 Y. M. Kuo, C. T. Wu, W. H. Wu and D. Y. Chao, *J. Appl. Polym. Sci.*, 1994, **52**, 1165–1173.
31 H. Yoshizawa, E. Kamio, N. Hirabayashi, J. Jacobson and Y. Kitamura, *J. Microencapsulation*, 2004, **21**, 241–249.
32 S. Tcholakova, N. D. Denkov and T. Danner, *Langmuir*, 2004, **20**, 7444–7458.
33 J. Rule, N. Sottos and S. White, *Polymer*, 2007, **48**, 3520–3529.

 This journal is © The Royal Society of Chemistry 2011